



## Soft x-ray resonant Kerr rotation measurement and simulation of element-resolved and interface-sensitive magnetization reversals in a Ni Fe/Fe Mn/Co trilayer structure

Sang-Koog Kim, Ki-Suk Lee, J. B. Kortright, and Sung-Chul Shin

Citation: [Applied Physics Letters](#) **86**, 102502 (2005); doi: 10.1063/1.1873047

View online: <http://dx.doi.org/10.1063/1.1873047>

View Table of Contents: <http://scitation.aip.org/content/aip/journal/apl/86/10?ver=pdfcov>

Published by the [AIP Publishing](#)

---

### Articles you may be interested in

[Magnetization reversal via symmetric rotation of layers in exchange biased multilayers](#)

J. Appl. Phys. **101**, 123913 (2007); 10.1063/1.2747539

[Magnetization reversal in single-layer and exchange-biased elliptical-ring arrays](#)

J. Appl. Phys. **97**, 10K113 (2005); 10.1063/1.1855461

[Influence of exchange bias coupling on the single-crystalline FeMn ultrathin film](#)

Appl. Phys. Lett. **86**, 122504 (2005); 10.1063/1.1883318

[Soft x-ray resonant magneto-optical Kerr effect as a depth-sensitive probe of magnetic heterogeneity: Its application to resolve helical spin structures using linear p polarization](#)

J. Appl. Phys. **96**, 7414 (2004); 10.1063/1.1806535

[Kerr effect observations of magnetization reversal process in antiferromagnetically pinned permalloy thin films](#)

J. Appl. Phys. **85**, 5525 (1999); 10.1063/1.369882

---

A banner for the 2014 Special Topics section of Applied Physics Letters. It features a central orange banner with the text '2014 Special Topics' in white. Below the banner are five circular icons representing different material categories: Perovskites, 2D Materials, Mesoporous Materials, Biomaterials/Bioelectronics, and Metal-Organic Framework Materials. The AIP logo and 'APL Materials' are on the left, and a red ribbon with 'Submit Today!' is on the right.

2014 Special Topics

PEROVSKITES

2D MATERIALS

MESOPOROUS MATERIALS

BIOMATERIALS/ BIOELECTRONICS

METAL-ORGANIC FRAMEWORK MATERIALS

AIP | APL Materials

Submit Today!

# Soft x-ray resonant Kerr rotation measurement and simulation of element-resolved and interface-sensitive magnetization reversals in a NiFe/FeMn/Co trilayer structure

Sang-Koog Kim<sup>a)</sup> and Ki-Suk Lee

Nanospintronics Laboratory, School of Materials Science and Engineering, and Research Institute of Advanced Materials, College of Engineering, Seoul National University, Seoul 151-744, Korea

J. B. Kortright

Materials Sciences Division, Lawrence Berkeley National Lab, One Cyclotron Road, Berkeley, California 94720

Sung-Chul Shin

Department of Physics, Korea Advanced Institute of Science and Technology, Daejeon 305-701, Korea

(Received 2 August 2004; accepted 7 January 2005; published online 2 March 2005)

We report experimental observations of element- and buried interface-resolved magnetization reversals in an oppositely exchange-biased NiFe/FeMn/Co trilayer structure by soft x-ray resonant Kerr rotation measurements. Not only Co-, Ni-, Fe-specific exchange-biased loops but also interfacial uncompensated (UC) Fe reversal loops coupled to the individual Co and NiFe layers are separately observed. From the experimental results interpreted with the help of the model simulations of soft x-ray resonant Kerr rotation, the effective thicknesses of interfacial UC regions at the buried interfaces of both FeMn/Co and NiFe/FeMn are found to be  $t_{UC} = 13 \pm 2$  Å and  $6 \pm 4$  Å, respectively. The depth sensitivity as well as element specificity of the x-ray resonant Kerr effect offer an elegant way into the investigations of element- and depth-resolved magnetization reversals of ferromagnetic ultrathin regions at buried interfaces in multicomponent multilayer films. © 2005 American Institute of Physics. [DOI: 10.1063/1.1873047]

The exchange bias effect observed in a variety of coupled ferromagnetic/antiferromagnetic (F/AF) systems has attracted much attention because of its fundamental interest<sup>1-9</sup> and technological applications to magnetic memory and sensor devices.<sup>10</sup> Its underlying physics has been debated for the past five decades.<sup>9,11</sup> According to the model suggested by Meiklejohn and Bean,<sup>1</sup> interfacial uncompensated (UC) AF spins in a close proximity of an F layer introduce a new class of magnetic anisotropy, i.e., unidirectional anisotropy into the F layer. In order to comprehensively understand unsolved issues regarding the exchange bias as well as discrepancies between the experimental and theoretical values of exchange bias field ( $H_{eb}$ ),<sup>3-5,9</sup> it is thus necessary to investigate separated magnetization **M** reversals of individual F and interfacial UC AF spins. However, detailed knowledge of the interfacial UC region in an AF layer is still lacking due to difficulties in the separate measurements of the interfacial region and the element-resolved reversals of individual magnetic constituents in multicomponent multilayer films.

In this letter, we report experimental observations of the element-resolved and depth-sensitive **M** reversals and their coupling in an oppositely exchange-biased NiFe/FeMn/Co structure, by employing soft x-ray resonant Kerr rotation ( $\theta_K$ ) measurements with varying incidence angle ( $\phi$ ) and photon energy ( $h\nu$ ). We have found that interfacial AF regions with its considerable thickness are ferromagnetic in character and coupled strongly to the individual NiFe and Co reversals, i.e., *switchable*. These UC regions are distinguishable from the interior of the nominal AF as well as F layers,

and hence their effective thicknesses can be estimated by comparing experimental reversal loops and those obtained by elaborate model simulations. These findings can offer a key insight into the exact underlying physics of exchange bias behaviors being under debates so far.<sup>3-5,9</sup>

The magnetic thin films studied here have two different F NiFe and Co layers separated by an AF FeMn layer. The two F layers are oppositely exchange-biased by the AF layer. Both interfacial UC AF regions were oppositely locked in while cooling through a typical blocking temperature of FeMn. The sample's layer structure is Si/SiO<sub>2</sub>(150 nm)/Ta(5 nm)/Ni<sub>81</sub>Fe<sub>19</sub>(8 nm)/Fe<sub>50</sub>Mn<sub>50</sub>

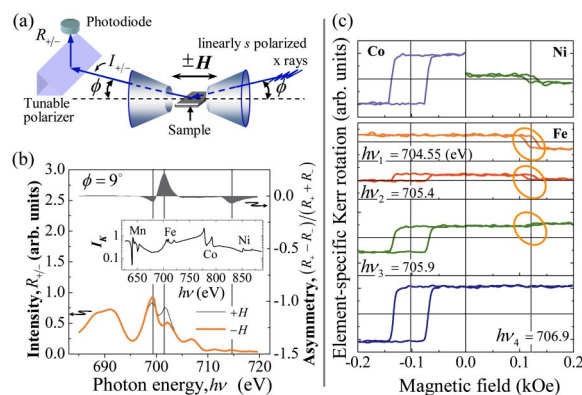


FIG. 1. (Color online) (a) An experimental geometry for the measurements of element-specific  $\theta_K$  with varying  $\phi$  and  $h\nu$ . (b)  $R_{\pm}$  as a function of  $h\nu$  in the vicinity of the Fe  $L_3$  and  $L_2$  edges from a tunable linear polarizer through reflections ( $I_K$ ) from the sample having a net **M** saturated along  $\pm H$ . The inset shows a spectrum of  $I_K$  measured at  $\phi = 9^\circ$  in the resonance regions of all the magnetic elements. Those  $h\nu$  values shown in (b) are not corrected. (c) Co-, Ni-, and Fe-resolved  $\theta_K$  loops measured at  $\phi = 9^\circ$  for Ni and Fe, and at  $\phi = 10^\circ$  for Co.

<sup>a)</sup> Author to whom all correspondence should be addressed; electronic mail: sangkoog@snu.ac.kr.

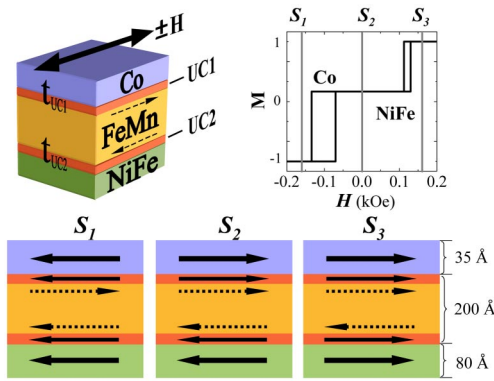


FIG. 2. (Color online) Model spin configurations at the representative magnetic fields noted by  $S_1$ ,  $S_2$ , and  $S_3$  in the F/AF/F trilayer of the real sample's layered structure. These spin configurations are assumed, according to the element resolved reversal loops shown in Fig. 1(c), to calculate Fe-specific  $\theta_K$  loops. The dashed arrows of antiparallel orientations near both F/AF interfaces indicate the unidirectional orientations of exchange bias locked in at the individual interfaces.

(20 nm)/Co(3.5 nm)/Pd(1.5 nm). Details of each layer growth, sample characterizations, and exchange bias setting will be reported elsewhere.<sup>12</sup> To investigate element-resolved and depth-sensitive  $\mathbf{M}$  reversals from that sample structure, we utilize an element-specific and depth-sensitive probe using synchrotron soft x rays and interpret those data with the help of elaborate model calculations.<sup>13,14</sup> The soft x-ray resonant magneto-optical  $\theta_K$  measurements were carried out by varying  $\phi$  and  $h\nu$  in the vicinity of the resonance regions of individual magnetic elements.

Figure 1(a) displays a geometry for the soft x-ray resonant  $\theta_K$  measurements using linearly  $s$ -polarized x rays at a chosen value of  $\phi$  and a tunable multilayer linear polarizer that senses the rotation of the plane of linear polarizations accompanying magnetic circular birefringence.<sup>15-17</sup> Co-, Ni-, and Fe-resolved loops were obtained through sufficiently large contrasts in the  $\theta_K$  signals by tuning  $h\nu$  as well as the linear polarizer to the corresponding resonance regions. Figure 1(b) displays how a large contrast of  $\theta_K$  for Fe-specific loops can be obtained using the tunable linear polarizer. The Kerr intensity ( $I_K$ ) from the sample having a saturation  $\mathbf{M}$  oriented along either direction of the longitudinal magnetic fields ( $\pm H$ ) were measured at  $\phi=9^\circ$  and in a  $h\nu$  range covering the Mn, Fe, Ni, and Co resonance edges, as shown in the inset of Fig. 1(b). The  $I_K$  spectrum reveals the resonant features of the individual elements in reflections, offering each element selectivity. The intensities ( $R_{+/-}$ ) from the sample through the linear polarizer under  $\pm H$  result from a superimposition of the variation of  $I_K$  and  $\theta_K$  for the sample together with a spectral reflectivity from the multilayer polarizer tuned around an Fe edge for strong reflections. The asymmetry ratio, defined as  $(R_+ - R_-)/(R_+ + R_-)$ , shows several peaks at the  $h\nu$  values noted by the vertical lines. This indicates that sufficiently large contrasts in  $\theta_K$  signals for opposite  $\mathbf{M}$  reversals can be obtained by tuning  $h\nu$  for the measurements of Fe-specific loops.<sup>18</sup> In addition to the element specificity, soft x-ray resonant Kerr effect has a much improved sensitivity to a specific depth region as well. This sensitivity also changes with  $h\nu$  and  $\phi$ . These novel properties can be utilized to resolve element-specific and depth-varying  $\mathbf{M}$  reversals in multicomponent multilayer films. Details for these measurements<sup>16,17</sup> and its related depth sensitivity<sup>13,14</sup> have been reported elsewhere.

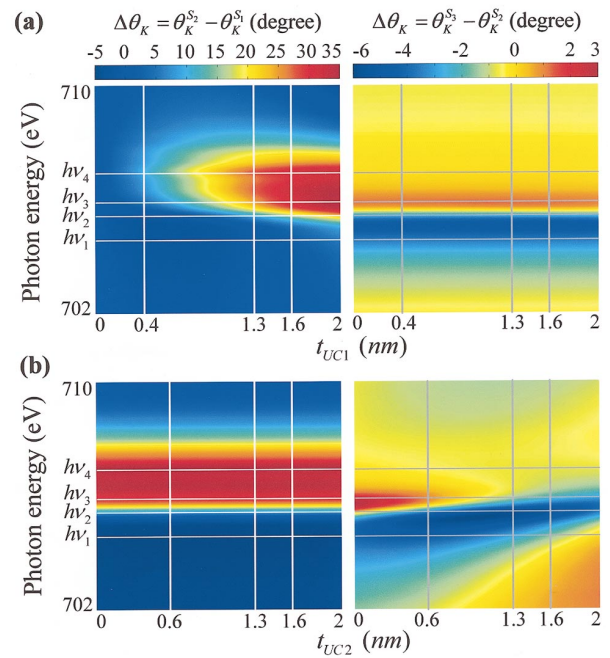


FIG. 3. (Color) (a) Contour plots of the calculated results of the Fe-resolved Kerr rotation contrasts  $\Delta\theta_K^{S_2-S_1}$  for a coupled UC1 and Co reversal and  $\Delta\theta_K^{S_3-S_2}$  for a coupled UC2 and NiFe reversal, with variable values of  $h\nu$  and  $t_{UC1}$  with keeping  $t_{UC2}=0.6$  nm in (a), and with  $h\nu$  and  $t_{UC2}$  while keeping  $t_{UC1}=1.3$  nm in (b). The horizontal lines note  $h\nu_1=704.55$ ,  $h\nu_2=705.4$ ,  $h\nu_3=705.9$ , and  $h\nu_4=706.9$  eV with a resolution of  $\pm 0.1$  eV which were selected in the Fe-specific  $\theta_K$  loop measurements. The vertical lines indicate  $t_{UC1}$  and  $t_{UC2}$  values used for model calculations of the Fe-resolved  $\theta_K$  loops to be shown in Fig. 4.

Figure 1(c) shows the resultant hysteresis loops of Co-, Ni-, and Fe-resolved  $\mathbf{M}$  reversals, measured via their element enhanced contrasts of  $\theta_K$  at the chosen values of  $h\nu$  as noted. From these results, we can identify individual  $\mathbf{M}$  switching behaviors of not only two F NiFe and Co layers but also interfacial UC regions in the nominal AF layer, and their correlations as well. The Co and Ni reversal loops are shifted to  $H_{eb}=-100$  and  $+120$  Oe, respectively, indicating that the two F layers are oppositely exchange-biased, as designed. It is strikingly interesting that positively or negatively or both side shifted loops of the Fe-resolved reversals are definitely observed depending on slightly different  $h\nu$  in the vicinity of the Fe  $L_3$  edge. The overall Fe Kerr signal in those Fe loops contributes from both the NiFe layer and the interfacial UC regions of the nominal AF layer. The negative and positive shifts of the Fe loops are exactly the same as  $H_{eb}=-100$  and  $+120$  Oe for the interfacial Co and the NiFe exchange bias, respectively.<sup>12,13</sup> It is evident from the negative side Fe loops that the interfacial UC Fe adjacent to the Co layer is F in character. Also, it is clear that this UC interfacial region is coupled strongly to the exchange-biased Co reversal, consequently switchable. As for the opposite side, the Fe loops originate from not only the F NiFe layer but also the interfacial UC region adjacent to the NiFe layer.<sup>19</sup> The two layers are also coupled at the FeMn/NiFe interface. Such strong coupling between the interfacial UC AF and F layers were also found in NiO/Co, IrMn/Co, and PtMn/CoFe films.<sup>9</sup>

Our next task is to determine the effective thicknesses of the switchable UC regions discriminated from the interior of the nominal AF layer. Both regions are denoted as UC1 and UC2 layers with their individual thicknesses,  $t_{UC1}$  and  $t_{UC2}$ , as shown in Fig. 2. The relative  $\mathbf{M}$  orientations of the indi-

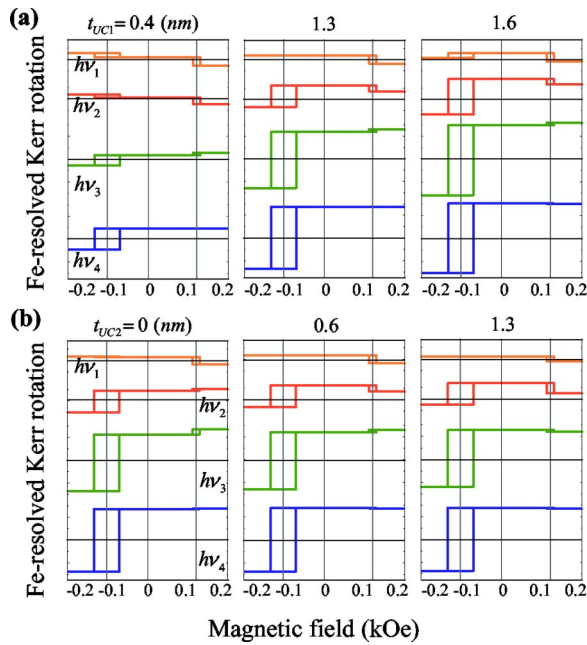


FIG. 4. (Color online) Comparison of the relative contrasts and polarities of the Fe-resolved loops, calculated for the noted values of  $h\nu$  and  $t_{UC1}$  with a fixed value of  $t_{UC2}=0.6$  nm in (a), and  $t_{UC2}$  with  $t_{UC1}=1.3$  nm in (b).

vidual UC1, UC2, Co, and NiFe layers are depicted for three different configurations ( $S_1$ ,  $S_2$ , and  $S_3$ ). In this model, the thicknesses of the Co and NiFe layers are kept to be the same as those of the real sample, but that of the AF FeMn layer is assumed to be reduced by the sum of  $t_{UC1}$  and  $t_{UC2}$ . Owing to an atomic-scale depth sensitivity of soft x-ray resonant Kerr effect varying remarkably with  $\phi$  and  $h\nu$ ,<sup>13,14</sup> the contrast and polarity of the observed Fe-resolved loops are contrasting depending on slightly different  $h\nu$ . A set of these loops is used to estimate  $t_{UC1}$  and  $t_{UC2}$  by adjusting the fit parameters of  $t_{UC1}$  and  $t_{UC2}$  in the calculations of soft x-ray  $\theta_K$  signals for various spin configurations.

Figure 3 shows contour plots of the calculated results of  $\Delta\theta_K^{S_2-S_1}$  and  $\Delta\theta_K^{S_3-S_2}$  variations with both  $h\nu$  and  $t_{UC1}$  with keeping a constant value of  $t_{UC2}=0.6$  nm in (a), and with both  $h\nu$  and  $t_{UC2}$  while keeping  $t_{UC1}=1.3$  nm in (b).  $\Delta\theta_K^{S_2-S_1}$  and  $\Delta\theta_K^{S_3-S_2}$  correspond to  $\theta_K$  contrasts for the simultaneous reversals of negatively exchange-biased Co and UC1 layers, and positively exchange-biased NiFe and UC2 layers, respectively, as shown in Fig. 2. The magnitude and sense of  $\Delta\theta_K$  for the two opposite exchange bias vary with both  $t_{UC1}$  and  $t_{UC2}$  as well as  $h\nu$ . It is found that the  $t_{UC1}$  variation leads to significant changes in the contrast and polarity of the negatively shifted Fe loops according to  $h\nu$ , while the variation of  $t_{UC2}$  primarily yields the change in those of the positively shifted Fe loops. Comparisons between experimentally observed and theoretically calculated  $\Delta\theta_K$  for different  $h\nu$  allow to determine both  $t_{UC1}$  and  $t_{UC2}$ . For instance, calculated Fe loops for the various values of  $t_{UC1}$  and  $t_{UC2}$  are shown in Fig. 4, from which those best fit values are found to be  $t_{UC1}=13\pm 2$  Å and  $t_{UC2}=6\pm 4$  Å, although the relative sizes of the calculated results of the negative side Fe loops for different  $h\nu$  disagree with experimental data.<sup>18</sup> It is worth noting that both  $t_{UC1}$  and  $t_{UC2}$  at buried interfaces are deter-

mined by the soft x-ray resonant  $\theta_K$  measurements together with their model calculations in the present work.

These found UC regions are magnetically distinct from the interior of the nominal AF layer and are thick enough to modify magnetic profiles in the trilayer sample, so that these regions can act as an additional buffer layer in exchange biasing. The magnetically distinct regions at AF/F interfaces can be formed due to the proximity effect in various hybrid systems.<sup>20,21</sup> For instance, a photoemission electron microscopy study revealed a chemical change at a Co/NiO interface.<sup>8</sup> Such proximity effect at F/AF interfaces and sufficiently large  $t_{UC}$  has been ignored in the explanation of significantly reduced experimental values of  $H_{eb}$ . Certainly, these regions can influence the size of  $H_{eb}$  and  $H_c$ , and hence must be explicitly considered in the development of theoretical models<sup>22</sup> of the exchange bias effect. To conclude, this work can offer a deeper insight into exchange bias behaviors. Furthermore, this probing technique is very useful in the investigations of element-resolved and depth-varying magnetization reversals multicomponent multilayer films.

This work was supported by the KOSEF through the q-Psi at Hanyang University and the BRP under Grant No. R08-2003-000-10410-0. Work at the ALS of LBNL was supported by the Director of the U.S. Department of Energy under Contract No. DE-AC03-76SF00098.

- <sup>1</sup>Meiklejohn and Bean, Phys. Rev. **102**, 1413 (1956); **105**, 904 (1957).
- <sup>2</sup>A. P. Malozemoff, Phys. Rev. B **35**, 3679 (1987).
- <sup>3</sup>D. Mauri, H. C. Siegmann, P. S. Bagus, and E. Kay, J. Appl. Phys. **62**, 3047 (1987).
- <sup>4</sup>K. Takano, R. H. Kodama, A. E. Berkowitz, W. Cao, and G. Thomas, Phys. Rev. Lett. **79**, 1130 (1997).
- <sup>5</sup>N. C. Koon, Phys. Rev. Lett. **78**, 4865 (1997).
- <sup>6</sup>W. J. Antel, Jr., F. Ferjeru, and G. R. Harp, Phys. Rev. Lett. **83**, 1439 (1999).
- <sup>7</sup>W. Zhu, L. Seve, R. Sears, B. Sinkovic, and S. S. P. Parkin, Phys. Rev. Lett. **86**, 5389 (2001).
- <sup>8</sup>H. Ohldag, T. J. Regan, J. Stöhr, A. Scholl, F. Nolting, J. Luning, C. Stamm, S. Anders, and R. L. White, Phys. Rev. Lett. **87**, 247201 (2001).
- <sup>9</sup>H. Ohldag, A. Scholl, F. Nolting, E. Arenholz, S. Maat, A. T. Young, M. Carey, and J. Stöhr, Phys. Rev. Lett. **91**, 017203 (2003).
- <sup>10</sup>G. A. Prinz, Science **282**, 1660 (1998).
- <sup>11</sup>J. Nogués and I. K. Schuller, J. Magn. Magn. Mater. **192**, 203 (1999).
- <sup>12</sup>Y.-S. Yu, K.-S. Lee, S.-K. Kim, K.-Y. Kim, S.-H. Jang, Y.-W. Kim, J.-W. Lee, and S.-C. Shin (unpublished).
- <sup>13</sup>K.-S. Lee, S.-K. Kim, and J. B. Kortright, Appl. Phys. Lett. **83**, 3764 (2003).
- <sup>14</sup>K.-S. Lee, D.-E. Jeong, S.-K. Kim, and J. B. Kortright (in press).
- <sup>15</sup>J. B. Kortright, M. Rice, and R. Carr, Phys. Rev. B **51**, 10240 (1995).
- <sup>16</sup>J. B. Kortright, M. Rice, S.-K. Kim, C. C. Walton, and T. Warwick, J. Magn. Magn. Mater. **191**, 79 (1999).
- <sup>17</sup>J. B. Kortright and S.-K. Kim, Phys. Rev. B **62**, 12216 (2000).
- <sup>18</sup>The sense and magnitude of  $\theta_K$  contrasts are found to be remarkably altered with  $\phi$  as well as  $h\nu$  in the vicinity of the resonance regions, which can lead to large variations of the size of  $\theta_K$  contrasts even with a  $h\nu$  variation of 0.2 eV.
- <sup>19</sup>In the model calculations, we considered which layers contribute to the positively shifted Fe loops. The simulated loops agree well with experimental results if both the NiFe and UC2 region are taken into account.
- <sup>20</sup>J. A. Borchers, M. J. Carey, R. W. Erwin, C. F. Majkrzak, and A. E. Berkowitz, Phys. Rev. Lett. **70**, 1878 (1993).
- <sup>21</sup>S.-K. Kim and J. B. Kortright, Phys. Rev. Lett. **86**, 1347 (2001).
- <sup>22</sup>K.-S. Lee, Y.-S. Yu, and S.-K. Kim (unpublished).